



FRACTAL AND WADA EXIT BASIN BOUNDARIES IN TOKAMAKS

JEFFERSON S. E. PORTELA and IBERÊ L. CALDAS
*Instituto de Física, Universidade de São Paulo,
C.P. 66318, 05315-970 São Paulo, Brazil*

RICARDO L. VIANA
*Departamento de Física, Universidade Federal do Paraná,
C.P. 19081, 81531-990 Curitiba, Paraná, Brazil*

MIGUEL A. F. SANJUÁN
*Nonlinear Dynamics and Chaos Group,
Departamento de Matemáticas y Física
Aplicadas y Ciencias de la Naturaleza,
Universidad Rey Juan Carlos,
Tulipán s/n, 28933 Móstoles, Madrid, Spain*

Received July 20, 2004; Revised November 15, 2006

The creation of an outer layer of chaotic magnetic field lines in a tokamak is useful to control plasma-wall interactions. Chaotic field lines (in the Lagrangian sense) in this region eventually hit the tokamak wall and are considered lost. Due to the underlying dynamical structure of this chaotic region, namely a chaotic saddle formed by intersections of invariant stable and unstable manifolds, the exit patterns are far from being uniform, rather presenting an involved fractal structure. If three or more exit basins are considered, the respective basins exhibit an even stronger Wada property, for which a boundary point is arbitrarily close to points belonging to *all* exit basins. We describe such a structure for a tokamak with an ergodic limiter by means of an analytical Poincaré field line mapping.

Keywords: Fractal basins; Wada basins; tokamaks; exit basins.

1. Introduction

One of the most important theoretical and experimental problems in fusion plasma research is the obtention of long-lasting plasma confinement through the application of suitable magnetic fields. The tokamak, one of the most promising candidates for a future fusion reactor, is a toroidal scheme in which the plasma current is confined by two main magnetic fields, one generated by external coils (*toroidal field*) and the other created by the plasma current itself (*poloidal field*) [Wesson, 1987]. The resulting magnetic field lines have helical shape,

and, as a consequence of magneto-hydrodynamical equilibrium, lie over constant pressure surfaces, or flux surfaces, which form nested tori [Meiss, 1992]. From the point of view of Hamiltonian dynamics, this can be viewed as an integrable system, thanks to the toroidal symmetry [Morrison, 2000]. However, the role of time here is to be played by the toroidal coordinate, since the configurations we are interested in are strictly magnetostatic.

This equilibrium can be substantially changed due to perturbing magnetic fields arising from both internal and/or external sources. There follows that, if the perturbation is weak enough, the topology of

the flux surfaces is significantly altered only at those surfaces exhibiting resonances with the perturbation. In these places there appear islands with the same dynamical structure of nonlinear pendula, and the corresponding Hamiltonian system has one and a half degrees of freedom [Lichtenberg & Lieberman, 1992]. Moreover, as a consequence of the breakup of integrability caused by the perturbation, we find chaotic motion limited to a thin layer surrounding the islands' separatrices. This chaotic layer can be enhanced by increasing the perturbation strength, and thus a mostly chaotic dynamics eventually sets in between adjacent resonances, according to the well-studied global stochasticity scenario [Chirikov, 1979].

We stress that chaotic motion is to be intended here in its Lagrangian sense: two magnetic field lines, which may be very close to one another at some point, diverge exponentially as they wind around the toroidal direction, with a rate given by the corresponding (positive) maximal Lyapunov exponent [Ott, 1993]. Moreover, identifying the flux surfaces as KAM tori of the corresponding Hamiltonian system, the existence of a chaotic region implies the breakup of flux surfaces. Hence, the chaotic magnetic field lines are volume-filling over a presumably limited extent of the tokamak torus [Meiss, 1992].

One can design the perturbing fields so as to create a wide chaotic region (in terms of the radial extent) near the plasma edge and the physical tokamak wall. There are sound reasons to do such a thing, the most important one being the role of a chaotic magnetic field as a divertor, in the sense that escaping particles and energy fluxes are spread out by the chaotic field, so reducing potentially harmful plasma-wall interactions [Engelhardt, 1977; Engelhardt & Feneberg, 1978]. This is the main goal of the so-called ergodic magnetic limiter, proposed in the late seventies and built in many research tokamaks [Karger & Lackner, 1977; Feneberg & Wolf, 1981].

Since the chaotic region is intended to extend from the plasma edge to the tokamak wall, it turns out that, once a plasma particle enters into this region, it will be driven outwards in an erratic fashion, and be eventually lost through collision with the tokamak wall [da Silva *et al.*, 2001]. Even though the chaotic region seems to uniformize those particle fluxes, the dynamic structures underlying the chaotic layer are complex enough to raise serious doubts about this claim. In fact, many available

experimental results point out that the tokamak wall is hit by plasma particles in a nonuniform way [Ohyabu *et al.*, 1984; Takamura *et al.*, 1989; Shen *et al.*, 1989; Wootton *et al.*, 1990; Araujo *et al.*, 1996].

The main point of this paper is that this nonuniformity can be traced out to the invariant manifold structure supporting the chaotic region, which has *escape channels* through which plasma particles are rapidly driven to the wall, forming *magnetic footprints* on it [Abdullaev *et al.*, 2002]. We call the set of initial conditions which eventually hit some portion of the wall the *escape basin* of that exit. The magnetic footprints should reflect in some sense the involved structure of the manifolds, like fractal boundaries separating different escape basins [Bleher *et al.*, 1988]. The presence of such escape boundaries has been observed in open Sinai billiards [Bleher *et al.*, 1988], advection of passive scalars in open fluid flows through an obstacle [Pentek *et al.*, 1995], and the motion of charged particles in Earth's magnetosphere [Chen, 1990].

If more than two exit possibilities are present, it follows that such escape basins can even exhibit the stronger *Wada property*: any point which is on the boundary of one escape basin is also simultaneously on the boundary of all the others [Nusse & Yorke, 1996a, 1996b]. One of the first examples of a set that possesses the Wada property was presented by Yoneyama [1917], who attributed the example to a certain Mr. Wada. In order to grasp the significance of the Wada property we may think of boundaries between countries in a (geographical) map. For example, there is a single point which is on the boundary of Brazil, Argentina and Paraguay (the *Three-frontier Landmark*). This is expected to occur for a finite number of boundary points, in general. However, if the Wada property would hold in such a case, there would be an uncountably infinite number of three-frontier landmarks between the three countries.

The Wada property has been extensively investigated in many open Hamiltonian systems, as the three-disk billiard [Poon *et al.*, 1996], particle scattering by a Hénon–Heiles potential [Aguirre *et al.*, 2001], including the limit of small exits [Aguirre & Sanjuán, 2003], light scattering by reflecting spheres [Sweet *et al.*, 1999], the advection of tracers in fluid flows [Toroczka *et al.*, 1997], and it was also studied in some “open” Hamiltonians maps by [Sanjuán *et al.*, 2003]. Moreover it has been also analyzed in dissipative systems such as in a quasi-periodically

driven system [Feudel *et al.*, 1999], the Duffing oscillator [Aguirre & Sanjuán, 2002], and the pendulum [Kennedy & Yorke, 1991; Nusse & Yorke, 1996b]. In the tokamak context, this problem has also been studied under the point of view of a chaotic scattering process [Abdullaev *et al.*, 2002; da Silva *et al.*, 2002]. This paper aims to describe the complex structure underlying the chaotic field line region, through identification of the Wada property in the escape basins of both the tokamak wall and obstacles, like divertor plates, placed in the chaotic region [Abdullaev *et al.*, 1998, 1999].

The rest of this paper is organized as follows: in Sec. 2, we review the theoretical background necessary to describe field line behavior in tokamaks, both in its geometrical and dynamical aspects. In particular, we show how an analytical map can be used to follow field line trajectories for a large number of revolutions around the tokamak torus. Section 3 is devoted to a description of exit (or escape) basins for field lines hitting both the tokamak wall and other obstacles. The fractal and Wada properties are described in Sec. 4, whereas the last section contains our conclusions.

2. Field Line Mapping in a Tokamak

The basic geometry of a tokamak is determined by its major (R_0) and minor (b) radii. When the tokamak aspect ratio R_0/b is large enough we can neglect, in a zeroth approximation, the effects of the toroidal curvature and treat it as a periodic cylinder of length $2\pi R_0$, whose axis of symmetry is parameterized by the coordinate $z = R_0\phi$ in terms of the toroidal angle ϕ (Fig. 1) [Wesson, 1987]. In this case, the equilibrium toroidal field B_0 is practically uniform. Accordingly, a point in the tokamak is located by its cylindrical coordinates (r, θ, z) with respect to that axis. On the other hand, in the study of the region nearby the tokamak wall, it turns out that even the poloidal curvature does not change results noticeably, so that a rectangular system can be found by defining the following coordinates: $x' = b\theta$ and $y' = b - r$ [Martin & Taylor, 1984]. The tokamak wall is thus characterized by the line segment $y' = 0$ extending from $x' = 0$ to $2\pi b$. In the following, we will use normalized coordinates $x = x'/b$ and $y = y'/b$.

The structure of the magnetic field lines in a tokamak can be more easily appreciated by taking a Poincaré surface of section at the plane $z = 0$. Let (r_n, θ_n) be the polar coordinates of the n th

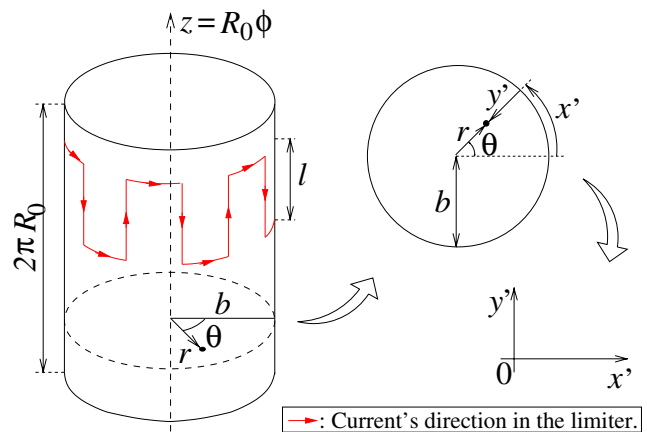


Fig. 1. Schematic view of the tokamak in the periodic cylinder approximation, its Poincaré section, and the rectangular coordinates (before normalization) used to describe magnetic field lines.

piercing of a given field line with that surface. Since the magnetic field line equations determine uniquely the position of the next piercing, we have a Poincaré map $(r_{n+1}, \theta_{n+1})^T = \mathbf{F}[(r_n, \theta_n)^T]$. Due to the solenoidal character of the magnetic field, this map is area-preserving in the surface of section [Morrison, 2000].

In the absence of any perturbation, the integrable configuration is described by a twist map $(r_n^*, \theta_n^*)^T = \mathbf{F}_1[(r_n, \theta_n)^T]$ [Ullmann & Caldas, 2000], where

$$r_n^* = \frac{r_n}{1 - a_1 \sin \theta_n}, \quad (1)$$

$$\theta_n^* = \theta_n + 2\pi\iota(r_n^*) + a_1 \cos \theta_n, \quad (2)$$

where $\iota(r)$ is the *rotational transform*, or the mean poloidal angle (over 2π) a field line sweeps after an entire toroidal revolution along the torus. There is a correction for the effect of the toroidal curvature which strength is represented by the a_1 parameter. In the following, we use $a_1 = -0.04$, according to [Ullmann & Caldas, 2000].

The dependence of the rotational transform with the radius is dictated by the details of the equilibrium magnetic field. The following expression describes in a satisfactory way plasma discharges in typical tokamak experiments [Caldas *et al.*, 2002]

$$\iota(r) = \frac{2\pi a^2}{q_a r^2} \left\{ 1 + \left[1 - \left(1 - \frac{r^2}{a^2} \right)^{\gamma+1} \right] \Theta(a - r) \right\}, \quad (3)$$

where a is the plasma radius (slightly less than the tokamak minor radius b), q_a and γ are parameters

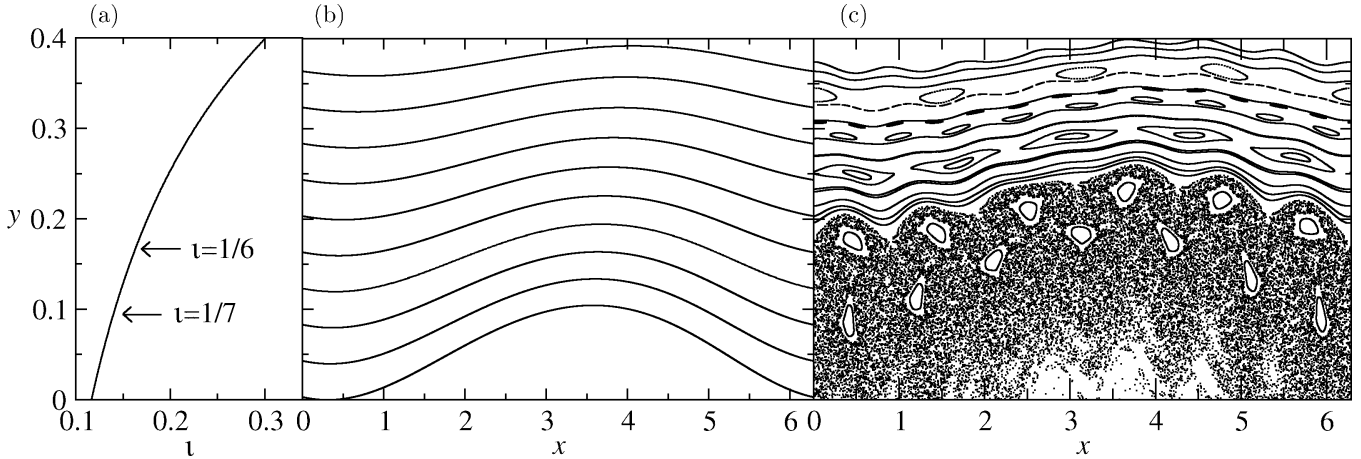


Fig. 2. (a) Radial profile of the equilibrium rotational transform at $x = 0$, in which the locations of the relevant resonance surfaces at the chaotic layer are indicated; (b) Phase portrait of a number of magnetic field lines in a Poincaré surface of section with no perturbation; (c) Same as (b), but with a $m = 7$ perturbation for which the ratio between the equilibrium plasma and limiter current is $I_h/I_p = 0.06$.

chosen to fit experimentally observed plasma profiles, and $\Theta(\cdot)$ is the unit step function. In Fig. 2(a) we plot the dependence of y with the rotational transform ι , indicating the radial position of magnetic surfaces with given values of their rotational transforms.

The ergodic limiter design we consider in this paper is a ring-shaped coil of width ℓ , with m pairs of straight pieces along the toroidal direction, with a current I_h flowing in opposite directions for two adjacent segments (Fig. 1) [Martin & Taylor, 1984; Caldas *et al.*, 1996; Portela *et al.*, 2003]. The effects of an ergodic limiter on such an equilibrium configuration can be approximated by a sequence of delta-function pulses at each piercing of a field line at the surface of a section. Such a mapping $(r_{n+1}, \theta_{n+1})^T = \mathbf{F}_2[(r_n^*, \theta_n^*)^T]$, has been described by Ullmann and Caldas [2000]:

$$r_n^* = r_{n+1} + \frac{mCb}{m-1} \left(\frac{r_{n+1}}{b}\right)^{m-1} \sin(m\theta_n^*), \quad (4)$$

$$\theta_n^* = \theta_n - C \left(\frac{r_{n+1}}{b}\right)^{m-2} \cos(m\theta_n^*), \quad (5)$$

where $C = mI_h\mu_0\ell/(\pi B_0b^2)$ represents the perturbation strength due to the magnetic ergodic limiter.

The entire field line mapping is the composition of the two mappings ($\mathbf{F} = \mathbf{F}_1 \circ \mathbf{F}_2$) and, since the variable r_{n+1} appears on both sides of the expression, we must solve it at each iteration using a numerical scheme (Newton–Raphson method). Nevertheless, the mapping \mathbf{F} is strictly area-preserving and can describe field line behavior in tokamaks with ergodic limiters in a convenient

and fast way, since we do not need to numerically integrate the field line equations over the whole toroidal revolution, in order to get the coordinates of a field line intersection with the Poincaré surface of section.

The equilibrium flux surfaces for the rotational transform profile of Fig. 2(a) are depicted in Fig. 2(b), where we plot a Poincaré surface of section of the magnetic field line flow without limiter action ($C = 0$), using the rectangular coordinates (x, y) defined at the beginning of this section. The flux surfaces intercept the surface of section as invariant (KAM) curves, with some shape distortion caused by the toroidicity effect ($a_1 \neq 0$). The effects of adding a nonintegrable perturbation such as that caused by an ergodic limiter are exemplified in Fig. 2(c), where we considered a ring-shaped limiter with $m = 7$ pairs of straight wires, the ratio between the limiter and plasma currents being $I_h/I_p = 0.06$.

Comparing Figs. 2(b) and 2(c) one recognizes the breaking of some flux surfaces, namely those with a rational value for the rotational transform (the *winding number* of the field lines), and the appearance of pendular island chains at the locations of the rational surfaces. Invariant curves still survive, according to the KAM theorem, provided they come from irrational surfaces [Lichtenberg & Lieberman, 1992]. A large chaotic region is clearly seen at the bottom of the phase portrait [Fig. 2(c)], indicating that many pendular islands (each of them with their own chaotic layer) have interacted forming a wide region of mainly chaotic

behavior, interspersed with isolated islands. This chaotic region was designed to be created near the tokamak wall at $y = 0$ by taking into account the fast decrease of the limiter field as we move towards the tokamak axis, when increasing the value of the y coordinate away from zero.

3. Exit Basins

In order to analyze the interaction between the chaotic region and the tokamak wall, we focus our attention on the escape pattern followed by field lines in this region. In a lowest order approximation (neglecting particle drifts) electrons and positive ions in a plasma will tend to follow magnetic field lines, and thus their structure gives us a first approach to the particle behavior in that region. Let us imagine that we select a bounded region *within* the chaotic region which an ergodic limiter generates near the tokamak wall. In this case, for a field line originating in this chaotic region there are two possibilities: (i) either the field line eventually escapes out of the tokamak by hitting its wall at $y = 0$; or (ii) the field line hits the bounded region first and is also considered as lost. These two possibilities may be considered as two exits

for trajectories of this near-integrable system. To be precise, there exists a Lebesgue measure zero set of initial conditions for which the trajectories never leave the chaotic region, but the probability of a typical trajectory to belong to this set is null [Grebogi *et al.*, 1983].

The exit (or escape) basin of a given exit is defined as the set of all initial conditions (in the chaotic region) which eventually leave the region through that exit [Bleher *et al.*, 1988]. In the situation we are considering in this paper, we can thus refer either to the exit basin of the tokamak wall, since it is considered as an exit region, or to the exit basin of a given region inside the chaotic layer. Figure 3(a) shows a phase portrait, in the Poincaré surface of section, where the perturbation parameters are the same as in Fig. 2(c), and there is a wide chaotic layer in the vicinity of the tokamak wall. The second exit (bounded region) is a small rectangular box placed at $x \approx 5.5$ and $y \approx 0.14$, with vertical and horizontal widths $w_y = 0.0045$ and $w_x = 20w_y$, respectively, and which apparently contains a large number of initial conditions in the chaotic region. The exit basin for it is pictured in green, whereas the exit basin for trajectories hitting the tokamak wall is painted in red. These two exit

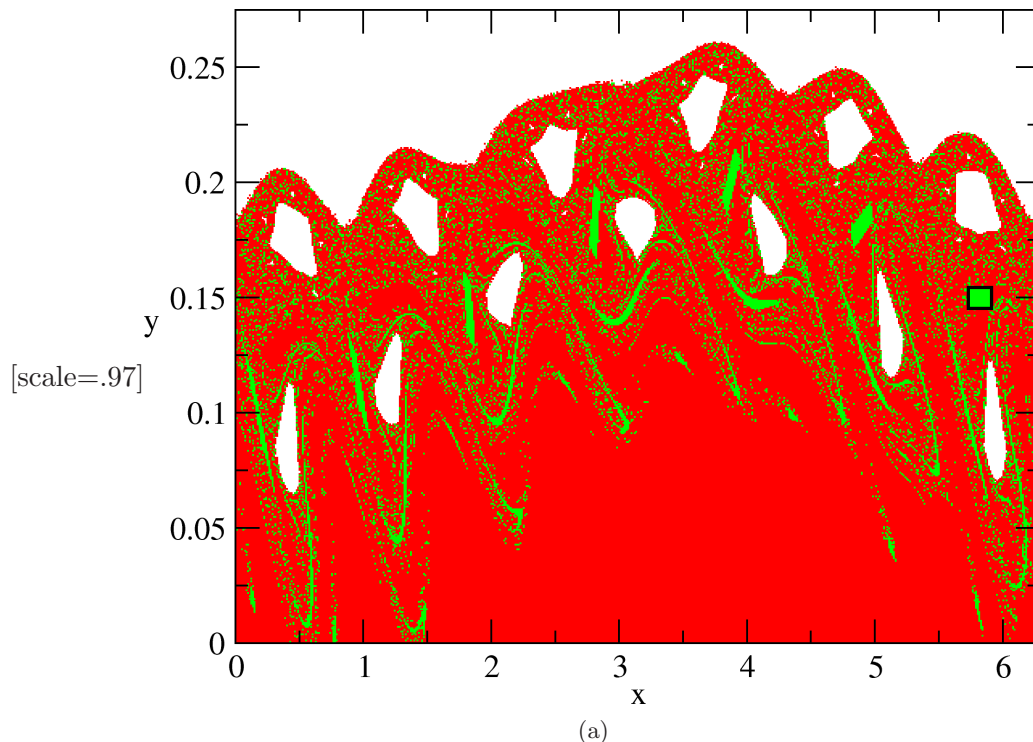


Fig. 3. Exit basins for orbits escaping through the tokamak wall (red) at $y = 0$, and through an exit (green) with width (a) $w_y = 0.0045$ and (b) $w_y = 0.0090$, with $w_x = 20w_y$. White regions are for orbits which never escape through either exit region. The limiter perturbation has $m = 7$ and $I_h/I_p = 0.06$.

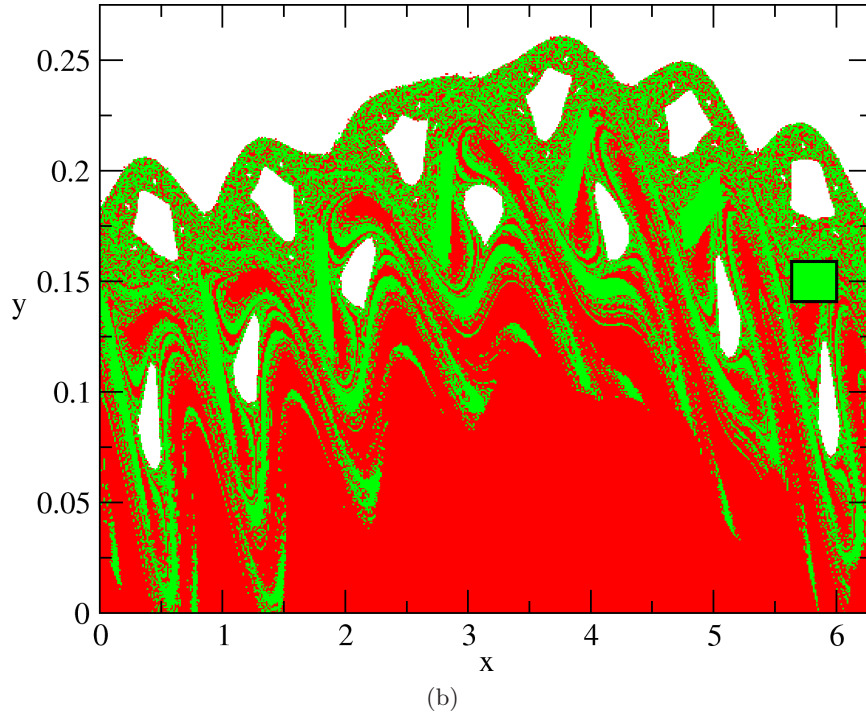


Fig. 3. (*Continued*)

basins have an extremely involved boundary, with a fractal nature revealed by the incursive structure present in finer scales.

The relative sizes of the two exit basins depend on the exit area, as revealed by Fig. 3(b), where the

vertical width has increased to $w_y = 0.0090$, the horizontal width being enlarged in the same proportion as before. The green basin has substantially augmented its relative area, with respect to the red basin.

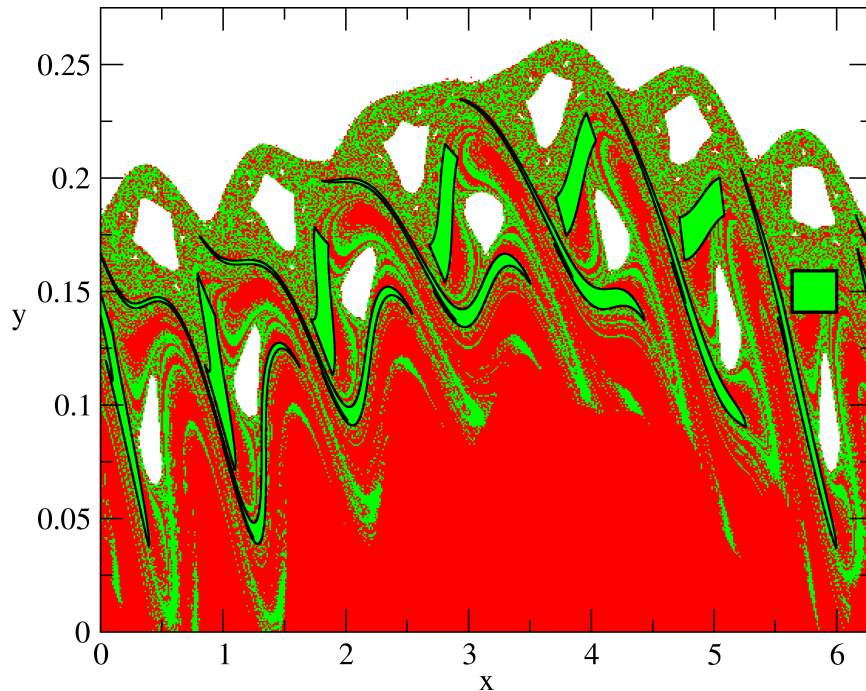


Fig. 4. Backward iterates of the rectangular box for which exit basins of field lines are painted green. The exit basin of the tokamak wall is painted red. Parameters are the same as in the previous figure.

The incursive fingers which characterize the exit basin of the small rectangular box in Fig. 4 are a consequence of the underlying dynamics of the chaotic region, governed by its invariant manifold structure. This can be observed by considering the inverse images, under the action of the mapping \mathbf{F} , of the small rectangular box in Fig. 4: it expands in one direction (roughly the radial one) and shrinks along the other direction. Such directions are provided by the unstable and stable manifolds, respectively, of unstable periodic orbits embedded in the chaotic region [Pentek *et al.*, 1995]. Chaotic trajectories are repelled along the unstable manifolds of such orbits. Since those manifolds intercept, in general, the tokamak wall at $y = 0$, almost all trajectories would eventually hit the wall, with the exception of a Lebesgue measure zero set of orbits.

However, if there is another obstacle, such as the small rectangular box in Fig. 4, trajectories will hit this exit before the wall, provided the unstable manifolds also intercept this rectangular box. The wider the exit is, the more unstable manifold segments will cross this exit, leading to trajectories escaping by that exit. Hence, the size of the exit influences the number of initial conditions which escapes through that exit; in other words, the size of its respective exit basin, as illustrated in Fig. 3. A small rectangular box in the chaotic region has a comparatively small exit basin [Fig. 3(a)], with respect to a wider rectangular box [Fig. 3(b)]. The influence of the exit size on the basin structure can be quantified by the uncertainty exponent technique to be discussed in the next section.

4. Fractal Exit Basin Boundaries

The exit basins depicted in Fig. 3 strongly suggest that the boundary separating two exit basins of a chaotic region has a fractal nature. The reason for this claim lies on the underlying structure of the chaotic region, or a *chaotic saddle*, formed by the intersections of the stable and unstable manifolds of an infinite number of unstable periodic orbits embedded in the chaotic region, and which support the ergodic measure of typical orbits [Grebogi *et al.*, 1988]. A chaotic saddle is a nonattracting invariant set with a dense chaotic orbit [Grebogi *et al.*, 1983]. Initial conditions belonging to this saddle are bound to remain in the chaotic region, unless portions of the saddle intercept the exit regions. In this case, even points in the chaotic saddle would eventually

escape. Nevertheless the Lebesgue measure of those exceptional initial conditions is zero. On the other hand, orbits originating from randomly chosen initial conditions usually wander in the vicinity of the chaotic saddle for a finite amount of time before escaping the chaotic saddle [Lai & Winslow, 1995].

Figure 5 shows the invariant stable and unstable invariant manifolds stemming from an unstable orbit (saddle point) embedded in the same chaotic region as that considered in previous figures. These manifolds were numerically obtained by considering the first 80 forward (backward) images of a small ball filled with a large number (5000×5000) of initial conditions and centered at a numerical approximation for the location of an unstable periodic orbit (saddle point) embedded in the chaotic orbit. There is a similarity between the striations displayed by the manifold branches and the incursive fingers characterizing pieces of the exit basins and which act as *escape channels* through which chaotic trajectories are pushed towards either the tokamak wall or another exit interposed in this region [da Silva *et al.*, 2002]. In Fig. 7 we show a numerical approximation of the chaotic saddle resulting from the intersection of the manifolds in Fig. 5.

The general mechanism responsible for the formation of the incursive fingers identified with such escape channels is illustrated in Fig. 6. Let P be an unstable periodic point of the map \mathbf{F} embedded in the chaotic region, with its respective stable (unstable) subspaces, denoted as $E^s(P)$ ($E^u(P)$). The eigenvalues corresponding to $E^s(P)$ and $E^u(P)$ are real and have moduli greater than and less than unity, respectively. These subspaces, on the other hand, are tangent to the stable ($W^s(P)$) and unstable ($W^u(P)$) manifolds at P . Let also A be a part of some exit basin, whose boundary is a partitioning line crossing the stable manifold of P . We assume also that the forward images of this region under the mapping, $\mathbf{F}^m(A)$, $m = 1, 2, 3, \dots$, also cross the stable manifold. These forward images approach the saddle point P such that they produce fingers which shrink along the direction of the stable manifold $W^s(P)$, with a rate equal to the corresponding eigenvalue of the tangent map in P . On the other hand, since the map \mathbf{F} is symplectic, in order to preserve areas these fingers will also elongate along the direction of the unstable manifold $W^u(P)$. As time goes to infinity, the fingers tend to accumulate in the unstable manifold itself, forming long and winding spaghetti-like striations which accompany $W^u(P)$ [Pentek *et al.*, 1995].

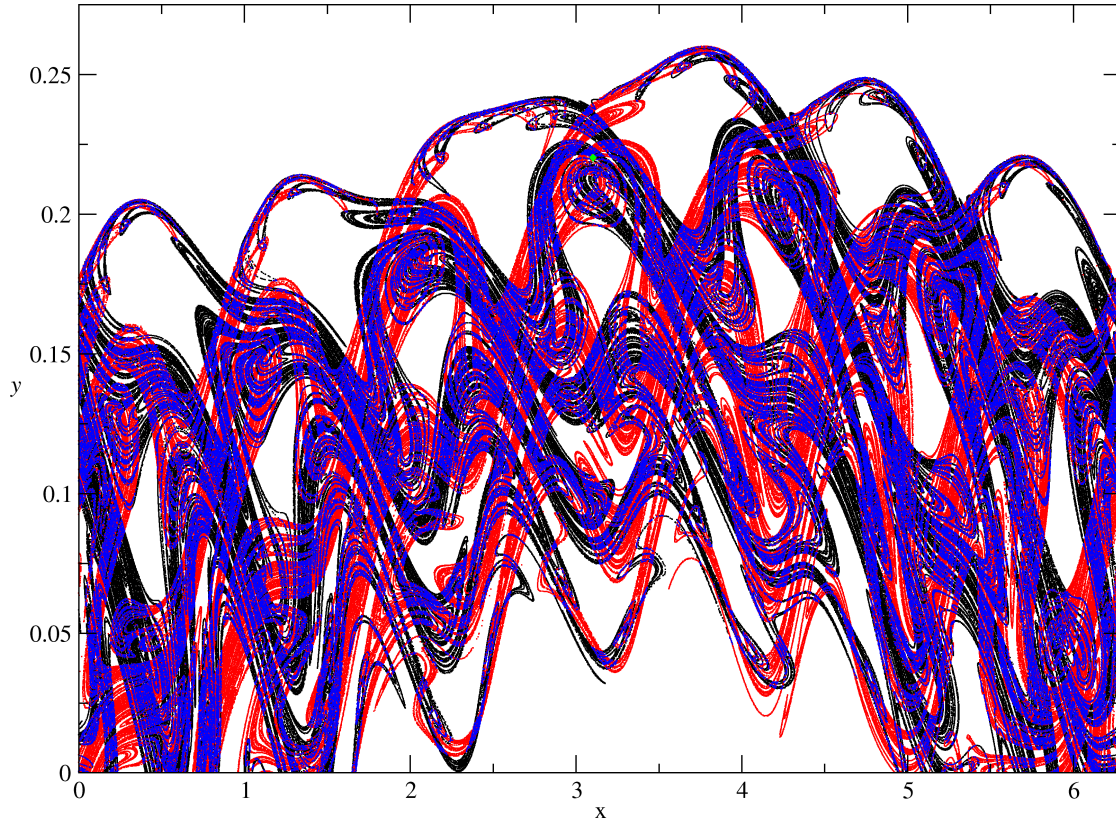


Fig. 5. Stable (black) and unstable (red) manifolds of an unstable periodic orbit (green) embedded in the chaotic region.

The same reasoning holds, *mutatis mutandis*, for the backward images of the $\mathbf{F}^{-m}(A)$, $m = 1, 2, 3, \dots$. Segments of the partitioning line lying between the filaments of the unstable manifold will be transported due to the backward dynamics and they will accumulate asymptotically on the

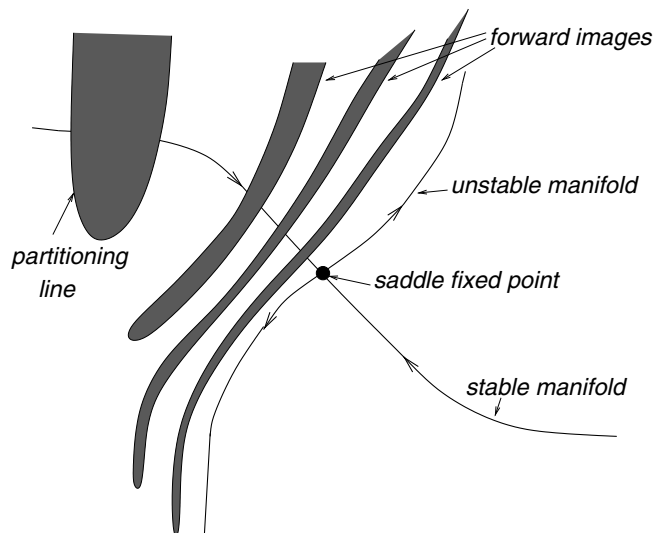


Fig. 6. Scheme showing the formation of the incursive fingers of the exit basin.

filaments of the stable manifold $W^s(P)$. Thus the boundary of the exit basins contains the stable and unstable manifolds of the chaotic saddle, or at least a part of them. It is necessary that the exit basin boundary crosses the invariant manifolds forming the chaotic saddle in order to have a fractal component. Moreover, since the fingers approaching the fixed point P extend smoothly along some manifold, this means that the exit basin boundary has also a smooth (nonfractal) component. Nevertheless, it is the fractal component of the exit basin boundary which is ultimately responsible for the formation of the escape channels and the corresponding nonuniformity of the magnetic footprints.

Fractal basin boundaries, such as those separating two exit basins, have final state sensitivity. Any initial condition is known up to a given uncertainty ϵ , such that we can think of a ball of radius ϵ centered at that initial condition. If the initial condition is so near the fractal boundary that the ϵ -ball does intercept the exit basin boundary, we cannot be sure if that initial condition will evolve to one or another exit. The union of all ϵ -balls intercepting the basin boundary gives the uncertain fraction (after dividing by the area of the phase space region

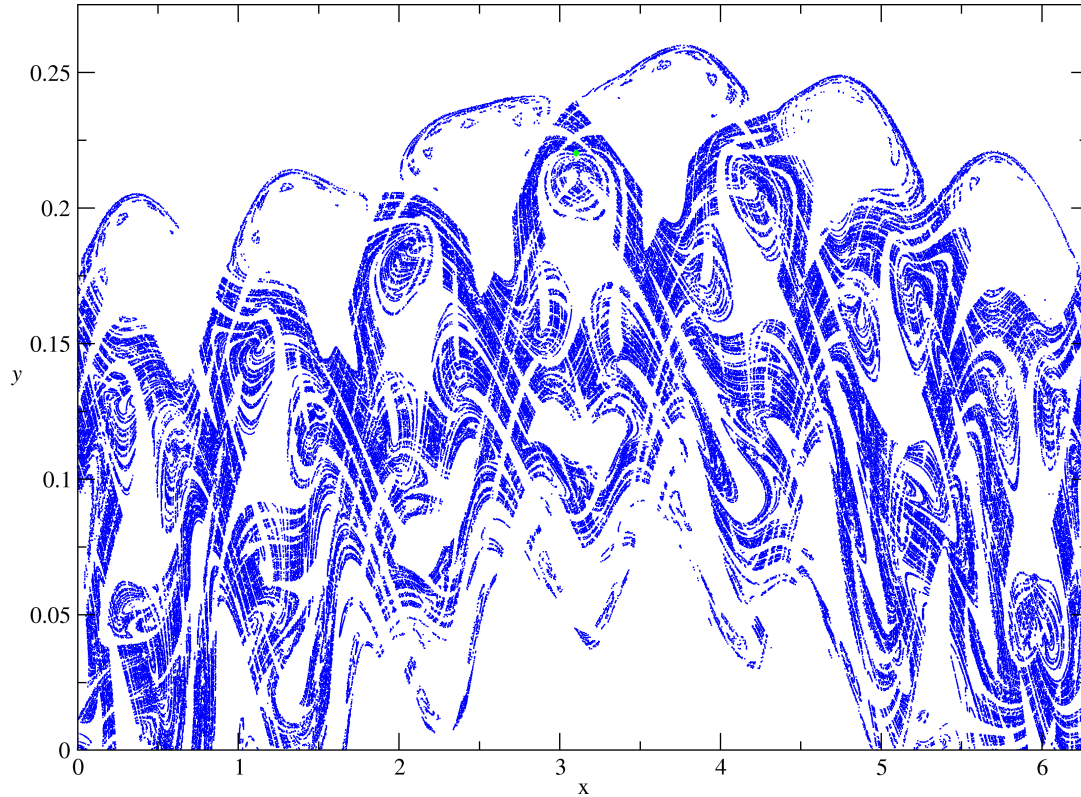


Fig. 7. Chaotic saddle formed by intersections of unstable and stable manifolds.

to be analyzed) $f(\epsilon)$. In fractal basin boundaries, the uncertain fraction scales in a power-law fashion with the uncertainty ball radius: $f(\epsilon) \sim \epsilon^\alpha$, where α is the uncertainty exponent. If d is the box-counting (fractal) dimension of the boundary, it follows that $\alpha = 2 - d$, since the surface of section is two-dimensional [McDonald *et al.*, 1985].

The more involved the basin boundary is, the higher is its box-counting dimension (i.e. closer to the phase plane dimension 2). Hence, d can be used as a quantitative characterization of the basin structure complexity. We can examine, for example, the influence of the exit width on the corresponding basin structure by computing the basin dimension through the uncertainty exponent method. We have selected a region comprising a representative portion of the exit basin boundaries in Fig. 3 and covered it with a fine mesh of initial conditions. At each initial condition \mathbf{A} we choose at random three other initial conditions \mathbf{B}_1 , \mathbf{B}_2 and \mathbf{B}_3 , inside an ϵ -ball centered at \mathbf{A} . If \mathbf{A} and $\mathbf{B}_{1,2,3}$ lead to orbits escaping through different exits, we call \mathbf{A} a ϵ -uncertain initial condition. The uncertain fraction was estimated from the ratio between the number of all uncertain conditions and the total number of them (the number of mesh points).

The uncertainty exponent was obtained from a least-squares fit in a log-log plot of $f(\epsilon)$ versus ϵ for different values of the exit width w_y (the other width is taken as an integer multiple $w_x = 20w_y$). Figure 8 shows our results for a series of different values of w_y . We can see a decrease in the

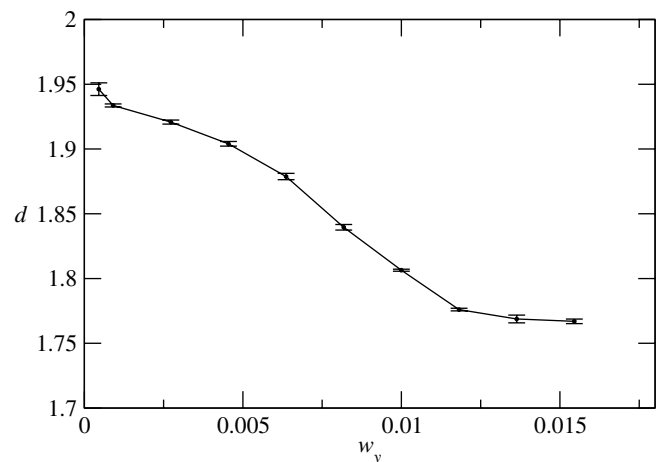


Fig. 8. Uncertainty dimension for the boundaries of the exit basins as a function of the exit width. Orbits escape either through the tokamak wall ($y = 0$) and a rectangular box centered at $(x = 3.1, y = 0.22)$ and widths w_y and $w_x = 20w_y$.

dimension of the basin boundary as the exit width is increased. Comparing Figs. 3(a) and 3(b) we conclude that, as the area of the exit basin increases, its boundary dimension decreases. Similar findings were reported on previous studies, where the escape rate was studied with respect to variations in the exit area [Schneider *et al.*, 2002; Sanjuan *et al.*, 2003].

5. Wada Exit Basin Boundaries

The Wada property has been also observed in the exit basin structure of magnetic field lines in a tokamak with ergodic limiter, when there are three or more exit basins. A point P is a boundary point of an exit basin \mathcal{B} if every open neighborhood of P intersects the basin \mathcal{B} and atleast another basin. The basin boundary is the set of all boundary points of that basin. Furthermore, the boundary point P is also a *Wada point* if every open neighborhood of P intersects at least three different basins. A basin boundary is said to possess the Wada property if every boundary point of \mathcal{B} is a Wada point, such that the boundary of such a basin is a *Wada exit basin boundary* [Nusse & Yorke, 1996a, 1996b].

In the plasma physics context of this paper, this is a striking phenomenon, since any boundary point is arbitrarily close to points of all exit basins [Kennedy & Yorke, 1991]. Since one initial condition is always known within some small nonzero uncertainty, this uncertainty ball will contain points of all exit basins. Hence, one has no previous certainty (however small the uncertainty ball may be) regarding which exit basin will the trajectory asymptote to. This means that no reliable forecasting can be made from boundary points possessing the Wada property, which limitates our knowledge of the situation.

An example of Wada boundary in tokamaks which has more than two exit basins is depicted in Fig. 9, where we painted the exit basins of two small rectangular boxes (in blue and green, respectively) and the tokamak wall (in red). The Wada property is strongly suggested by successive magnification of a rectangle containing pieces of the three exit basins [Fig. 9(b)]. Further magnifications enhance this effect, since stripes of all basins coexist in finer scales [Fig. 9(c) and 9(d)]. Similar results appear when we divide the tokamak wall into different regions and consider them as the exits, so as to assign a given exit basin to each region [da Silva *et al.*, 2002].

There is, however, a more precise identification of the Wada property that can be used in this context. A necessary, albeit not sufficient condition for a given exit basin boundary to possess the Wada property is that the unstable manifold $W^u(P)$ of an unstable periodic orbit P belonging to this boundary must intersect every exit basin. We have verified explicitly the necessary condition for the existence of exit basin boundaries with the Wada property, by considering in Fig. 9(b) (in yellow) a piece of the unstable manifold stemming from a saddle point belonging to an exit basin boundary. This manifold piece clearly intercepts points of the red, green and blue basins, hence the unstable manifold of a periodic orbit P belonging to an exit basin boundary has intersected all the exit basins.

In order that a basin boundary possesses the Wada property, at least one of the complementary conditions below has to be satisfied [Kennedy & Yorke, 1991; Nusse & Yorke, 1996]: (i) the stable manifold of the point P must be dense in the boundary of the three regions; (ii) the periodic orbit P must be the only accessible orbit from the exit basin \mathcal{B} . Otherwise, every unstable manifold of other periodic orbits that are accessible from \mathcal{B} must intersect all basins. We say that a boundary point P is accessible from a particular basin if there is another point in the interior of the basin which can be connected to P by a finite length curve that contains no boundary points except P [Poon *et al.*, 1996]; (iii) the periodic orbit P must generate a basin cell. A cell is a region with a piecewise smooth boundary, whose edges are alternately pieces of stable and unstable manifolds of a periodic orbit. A basin cell is a cell that is a trapping region [Nusse & Yorke, 1996b].

The direct numerical verification of these complementary conditions turns out to be rather difficult, so that we used another argument of checking the Wada property for the exit basin boundaries in this work; and which consists of verifying that every open neighborhood of a boundary point intersects all exit basins [Toroczkai *et al.*, 1997]. The reason for this claim is the following [Toroczkai *et al.*, 1997]: let us take a point P on the exit boundary, which is actually the stable manifold of some periodic orbit containing the point P . We take a small ball \mathcal{D} of initial conditions centered at P , and compute its forward images under the mapping, $\mathbf{F}^m(\mathcal{D})$. As m increases the image of \mathcal{D} becomes a convoluted and very thin ribbon extending along the unstable manifold of P , as can be observed in Fig. 5.

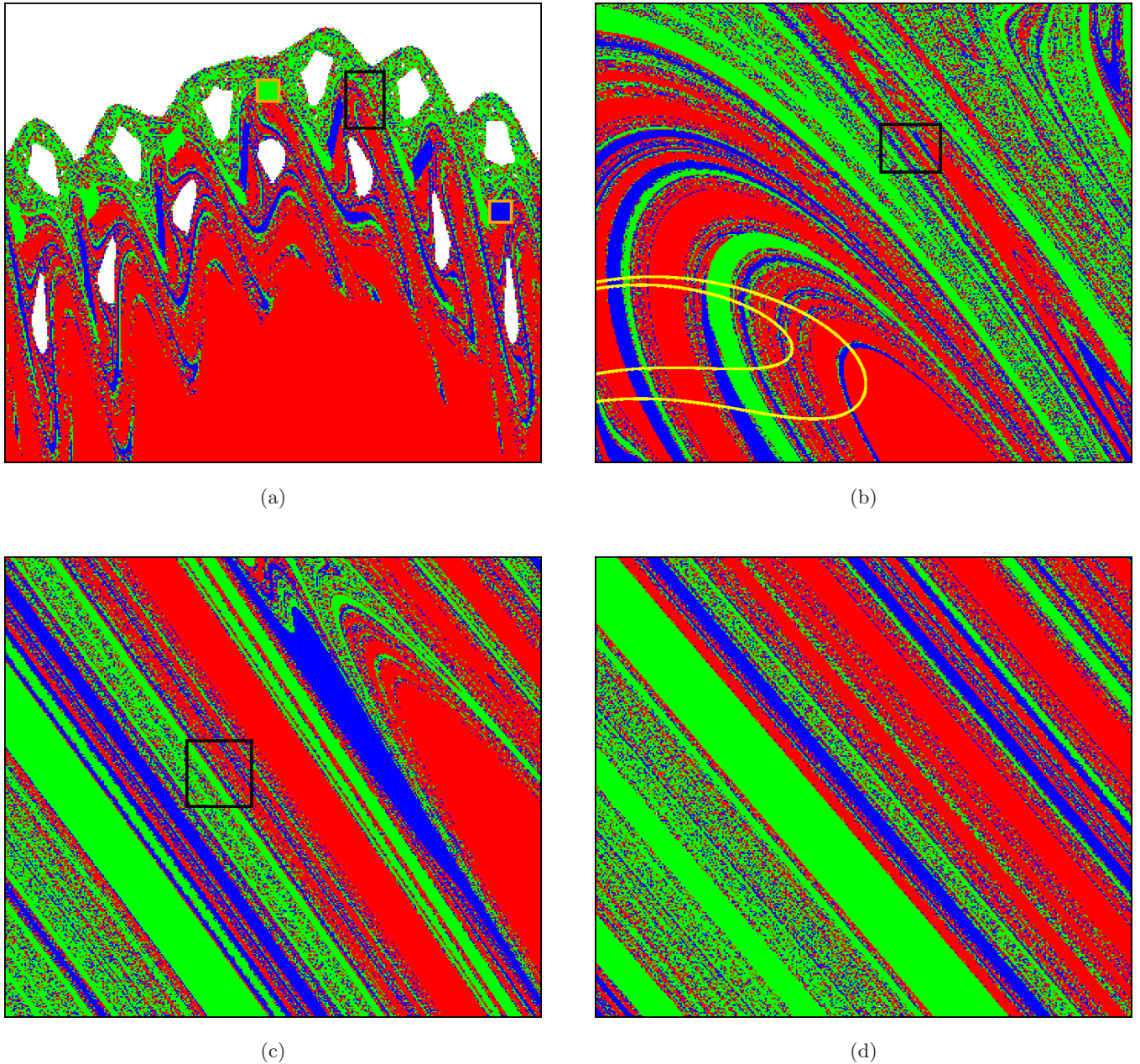


Fig. 9. (a) Exit basins for orbits escaping through the tokamak wall (red) and two small rectangular boxes (green and blue, respectively) with orange borders. (b)–(d) successive magnifications of rectangular boxes with black borders. The yellow line in (b) is a numerical approximation of the part of the unstable manifold of an unstable orbit embedded in the chaotic layer.

The ball \mathcal{D} is a connected set, and so are its images under the mapping \mathbf{F} . Consider now that there is a finite value of $m = m_0$ such that $\mathbf{F}^{m_0}(\mathcal{D})$ intersects all the exit basins (as shown in Fig. 9). Because $\mathbf{F}^{m_0}(\mathcal{D})$ maps to \mathcal{D} under m_0 backward iterations, all the basin structures present in $\mathbf{F}^{m_0}(\mathcal{D})$ are also mapped into \mathcal{D} . Since we did not make any particular assumption about the radius of \mathcal{D} , and since the point P can be anywhere on the stable manifold, this statement is valid for all

radii (whenever small), such that the entire stable manifold is a Wada exit basin boundary.

The reasoning we presented in the previous section leads to the conclusion that the exit basins closely follow the invariant manifold structure underlying the dynamics in the chaotic region. The exit basin boundaries are, thus, made of parts of invariant manifolds stemming from unstable periodic orbits (saddles in two dimensions) embedded in the chaotic region. The fingerprint of the Wada

property is the fact that the stable manifold of an orbit belonging to the basin boundary intercepts pieces of all exit basins.

6. Conclusions

We have described in this paper topological properties of exit basins which have potential applications in the design of experiments aiming to make uniform the plasma-wall interactions in tokamaks. The original belief was that a chaotic layer of magnetic field lines could spread particle and energy fluxes uniformly towards the tokamak wall. Further experiments suggested that this would not be necessarily so. Actually this nonuniformity may be a consequence of the escape channels which appear due to the extremely involved nature of stable and unstable manifolds embedded in the chaotic region.

The magnetic footprints on the tokamak wall (or, in general, on any obstacle placed in the chaotic region) are thus strongly affected by the fractal nature of the chaotic saddle underlying the chaotic region. Besides the fractal character, there are also Wada boundaries, for which any boundary point is arbitrarily close to points of all exit basins (when there are at least three of them). This makes for an extremely intertwined structure of basin pieces, such that it may be virtually unfeasible to make any kind of prediction regarding what exit basin a given initial condition will asymptote to, since such initial conditions are known only up to a finite precision.

For a practical application of this fact, let us suppose that an experimentalist would like to inject a particle beam in the plasma region dominated by a chaotic magnetic field, such that the beam is targeted at a given region of the tokamak wall or another obstacle, like the rectangular boxes in Fig. 9. Due to the extremely involved nature of the basin structure when the Wada property is present, it is very difficult to make reliable predictions about the behavior of the beam, as long as the particles which gyrate around magnetic field lines, thus disregarding drifts caused by field nonhomogeneities and curvatures [Chen, 1984].

The main purpose of this paper was to investigate topological properties related to the exit basins. It would be also possible to study this situation through a metric approach, computing escape rates and times, in order to quantify chaotic transport of magnetic field lines in the edge region of the tokamak, and for which there exists a number of rigorous results [Meiss, 1992].

Acknowledgments

This work was made possible through partial financial support from the following Brazilian research agencies: FAPESP and CNPq. MAFS acknowledges financial support from the Spanish Ministry of Science and Technology under project BFM2003-03081. The authors would like to acknowledge Professor Celso Grebogi for valuable discussions and useful suggestions.

References

- Abdullaev, S. S., Finken, K. H., Kaleck, A. & Spatschek, K. H. [1998] "Twist mapping for the dynamics of magnetic field lines in a tokamak ergodic divertor," *Phys. Plasmas* **5**, 196–210.
- Abdullaev, S. S., Finken, K. H. & Spatschek, K. H. [1999] "Asymptotical and mapping methods in study of ergodic divertor magnetic field in a toroidal system," *Phys. Plasmas* **6**, 153–174.
- Abdullaev, S. S., Eich, Th. & Finken, K. H. [2001] "Fractal structure of the magnetic field in the laminar zone of the dynamic ergodic divertor of the torus experiment for technology-oriented research (TEXTOR-94)," *Phys. Plasmas* **8**, 2739–2749.
- Aguirre, J., Vallejo, J. C. & Sanjuán, M. A. F. [2001] "Wada basins and chaotic invariant sets in the Hénon–Heiles system," *Phys. Rev. E* **64**, 066208.
- Aguirre, J. & Sanjuán, M. A. F. [2002] "Unpredictable behavior in the Duffing oscillator: Wada basins," *Physica D* **171**, 41–51.
- Aguirre, J. & Sanjuán, M. A. F. [2003] "Limit of small exits in open Hamiltonian systems," *Phys. Rev. E* **67**, 056201.
- Araújo, M. S. T., Vannucci, A. & Caldas, I. L. [1996] "Observation of disruptions in tokamak plasma under the influence of resonant helical magnetic fields," *Nuovo Cim. D* **18**, 807–821.
- Bleher, S., Grebogi, C., Ott, E. & Brown, R. [1988] "Fractal boundaries for exit in Hamiltonian dynamics," *Phys. Rev. A* **38**, 930–938.
- Bleher, S., Grebogi, C. & Ott, E. [1990] "Bifurcation to chaotic scattering," *Physica D* **46**, 87–121.
- Caldas, I. L., Pereira, J. M., Ullmann, K. & Viana, R. L. [1996] "Magnetic field line mappings for a tokamak with ergodic limiters," *Chaos Solit. Fract.* **7**, 991–1010.
- Caldas, I. L., Viana, R. L., Araujo, M. S. T., Vannucci, A., da Silva, E. C., Ullmann, K. & Heller, M. V. A. P. [2002] "Control of chaotic magnetic fields in tokamaks," *Braz. J. Phys.* **32**, 980–1004.
- Chen, F. F. [1984] *Introduction to Plasma Physics and Controlled Fusion*, 2nd edition (Plenum Press, NY & London).

- Chen, J., Rexford, J. L. & Lee, Y. C. [1990] “Fractal boundaries in magnetotail particle dynamics,” *Geophys. Res. Lett.* **17**, 1049–1052.
- Chirikov, B. [1979] “A universal instability of many-dimensional oscillator systems,” *Phys. Rep.* **52**, 265–379.
- da Silva, E. C., Caldas, I. L. & Viana, R. L. [2001] “Field line diffusion and loss in a tokamak with an ergodic magnetic limiter,” *Phys. Plasmas* **8**, 2855–2865.
- da Silva, E. C., Caldas, I. L., Viana, R. L. & Sanjuán, M. A. F. [2002] “Escape patterns, magnetic footprints, and homoclinic tangles due to ergodic magnetic limiters,” *Phys. Plasmas* **9**, 4917–4928.
- Engelhardt, W. & Feneberg, W. [1978] “Influence of an ergodic magnetic limiter on the impurity content in a tokamak,” *J. Nucl. Mat.* **76/77**, 518–520.
- Feneberg, W. [1977] “The use of external helical windings for the production of a screening layer in ASDEX and a Tokamak with a material limiter,” *Proc. Eighth European Conf. Controlled Fusion and Plasma Physics*, ed. Petit-Lancy, Vol. 1 (European Physical Society), p. 3.
- Feneberg, W. & Wolf, G. H. [1981] “A helical magnetic limiter for boundary-layer control in large tokamaks,” *Nucl. Fus.* **21**, 669–676.
- Feudel, U., Witt, A., Lai, Y.-C. & Grebogi, C. [1998] “Fractal and Wada basin boundaries in quasiperiodically driven systems,” *Phys. Rev. E* **58**, 3060–3066.
- Grebogi, C., Ott, E. & Yorke, J. A. [1983] “Crises, sudden changes in chaotic attractors, and transient chaos,” *Physica D* **7**, 181–200.
- Grebogi, C., Ott, E. & Yorke, J. A. [1988] “Unstable periodic orbits and the dimensions of multifractal chaotic attractors,” *Phys. Rev. E* **37**, 1711–1724.
- Karger, F. & Lackner, K. [1977] “Resonant helical diverter,” *Phys. Lett. A* **61**, 385.
- Kennedy, J. & Yorke, J. A. [1991] “Basins of Wada,” *Physica D* **51**, 213–225.
- Lai, Y. C. & Winslow, R. L. [1995] “Geometric properties of the chaotic saddle responsible for supertransients in spatiotemporal chaotic systems,” *Phys. Rev. Lett.* **74**, 5208–5211.
- Lichtenberg, A. J. & Leiberman, M. A. [1992] *Regular and Chaotic Dynamics*, 2nd edition (Springer-Verlag, NY-Berlin-Heidelberg).
- Martin, T. J. & Taylor, J. B. [1984] “Ergodic behavior in a magnetic limiter,” *Plas. Phys. Contr. Fus.* **26**, 321.
- McDonald, S. W., Grebogi, C., Ott, E. & Yorke, J. A. [1985] “Fractal basin boundaries,” *Physica D* **17**, 125–153.
- Meiss, J. D. [1992] “Symplectic maps, variational principles, and transport,” *Rev. Mod. Phys.* **64**, 795–848.
- Morrison, P. J. [2000] “Magnetic field lines, Hamiltonian dynamics, and nontwist systems,” *Phys. Plasmas* **7**, 2279–2289.
- Nusse, H. E. & Yorke, J. A. [1996a] “Basins of attraction,” *Science* **271**, 1376–1380.
- Nusse, H. E. & Yorke, J. A. [1996b] “Wada basin boundaries and basin cells,” *Physica D* **90**, 242–261.
- Ohyabu, N., deGrassie, J. S., Brooks, N. H., Taylor, T. S. & Ikezi, H. [1984] “Preliminary results from the ergodic magnetic limiter experiment on the TEXT experimental tokamak,” *J. Nucl. Mat.* **121**, 363–367.
- Ott, E. [1993] *Chaos in Dynamical Systems* (Cambridge University Press, NY).
- Péntek, A., Toroczkai, Z., Tél, T., Grebogi, C. & Yorke, J. A. [1995] “Fractal boundaries in open hydrodynamical flows: Signatures of chaotic saddles,” *Phys. Rev. E* **51**, 4076.
- Poon, L., Campos, J., Ott, E. & Grebogi, C. [1996] “Wada basin boundaries in chaotic scattering,” *Int. J. Bifurcation and Chaos* **6**, 251–265.
- Portela, J. E. S., Viana, R. L. & Caldas, I. L. [2003] “Chaotic magnetic field lines in tokamaks with ergodic limiters,” *Physica A* **317**, 411–431.
- Roberto, M., da Silva, E. C., Caldas, I. L. & Viana, R. L. [2004] “Magnetic trapping caused by resonant perturbations in tokamaks with reversed magnetic shear,” *Phys. Plasmas* **11**, 214–225.
- Sanjuán, M. A. F., Horita, T. & Aizara, H. [2003] “Opening a closed Hamiltonian map,” *Chaos* **13**, 17–24.
- Schneider, J., Tel, T. & Neufeld, Z. [2002] “Dynamics of ‘leaking’ Hamiltonian systems,” *Phys. Rev. E* **66**, 066218.
- Shen, S., Miyake, S. M., Takamura, S., Kuroda, T. & Okuda, T. [1989] “Ergodic magnetic limiter experiments in the HYBTOK-II tokamak,” *J. Nucl. Mat.* **168**, 295–303.
- Sweet, D., Ott, E. & Yorke, J. A. [1999] “Complex topology in chaotic scattering: A laboratory observation,” *Nature* **399**, 315.
- Takamura, S., Shen, Y., Yamada, H., Miyake, M., Tamakoshi, T. & Okuda, T. [1989] “Electric and magnetic structure of tokamak edge plasma with static and rotating helical magnetic limiter,” *J. Nucl. Mat.* **162–164**, 643–647.
- Toroczkai, Z., Károlyi, G., Péntek, A., Tél, T., Grebogi, C. & Yorke, J. A. [1997] “Wada dye boundaries in open hydrodynamical flows,” *Physica A* **239**, 235–243.
- Ullmann, K. & Caldas, I. L. [2000] “A symplectic mapping for the ergodic magnetic limiter and its dynamical analysis,” *Chaos Solit. Fract.* **11**, 2129–2140.
- Wesson, J. [1987] *Tokamaks* (Oxford University Press, Oxford, 1987).
- Wootton, A. J., Carreras, B. A., Matsumoto, H., McGuire, K., Peebles, W. A., Ritz, Ch. P., Terry, P. W. & Sweben, S. J. [1990] “Fluctuations and anomalous transport in tokamaks,” *Phys. Plasmas* **2**, 2879–2903.
- Yoneyama, K. [1917] “Theory of continuous sets of points,” *Tohoku Math. J.* **11–12**, 43.